energies

MDPI

Article

Performance Evaluation of a Hybrid Grid-Connected Photovoltaic Biogas-Generator Power System

Heyam Al-Najjar [1,*], Christoph Pfeifer [1,*], Rafat Al Afif [1] and Hala J. El-Khozondar [2]

[1] Institute of Chemical and Energy Engineering, University of Natural Resources and Life Sciences, Muthgasse 107, 1190 Vienna, Austria; rafat.alafif@boku.ac.at
[2] Electrical Engineering and Smart Systems Department, Islamic University of Gaza, Gaza Strip P.O. Box 108, Palestine; hkhozondar@iugaza.edu
* Correspondence: heyam.k-j-alnajjar@students.boku.ac.at (H.A.-N.); christoph.pfeifer@boku.ac.at (C.P.)

Abstract: In recent decades, works have been published on the Hybrid Renewable Energy System (HRES) to provide available, feasible, and efficient renewable energy systems. Several studies have looked at the efficiency of the systems in terms of sustainability through performance parameters. This study aims at estimating the optimum HRES based on biomass and photovoltaic (PV) using the case study of 94 residential buildings with an electricity demand of 84.5 kWp. The influence of key parameters (global solar irradiation, component efficiencies, fuel consumption, economic convenience) and their impact on the performance and cost of the system is investigated. The optimum system is evaluated by the simulation software HOMER Pro. A single year of hourly data is used to analyze the component performance and the overall system performance. In this work, a mathematical model based on the IEC 61724 standard is used to incorporate numerous performance indicators that are critical for estimating the performance of a hybrid system. Evaluating results comprise of three performance basic indicators, namely, energy efficiency, system sizing, and economic parameters.

Keywords: grid-tied hybrid energy system; renewable energy; photovoltaic; biogas; mathematical modelling; performance evaluation; specific fuel consumption; balance of system; normalized performance parameters

check for updates

Citation: Al-Najjar, H.; Pfeifer, C.; Al Afif, R.; El-Khozondar, H.J. Performance Evaluation of a Hybrid Grid-Connected Photovoltaic Biogas-Generator Power System. *Energies* **2022**, *15*, 3151. https://doi.org/10.3390/en15093151

Academic Editors: John Gardner, Seongjin Lee, Kee Han Kim and Sukjoon Oh

Received: 14 March 2022
Accepted: 18 April 2022
Published: 26 April 2022

1. Introduction

Since solar energy is unlimited and clean, it can provide a feasible and long-term solution to the problem of excessive energy consumption. Photovoltaic (PV) generators can harvest and convert this energy directly to electricity [1]. Accordingly, solar energy is widely found in hybrid systems, as suggested by several research groups [2–4]. PV and biomass energy sources could be combined in a grid-tied or grid-off hybrid system. In such a microgrid, the technology applied to convert biomass to electricity is dependent on the plant size. Biogas is gathered from biomass in a process called anaerobic digestion, and then it is used to produce electricity via gas engines or even turbines as its average calorific value is between 21 and 23.5 MJ/m^3 (6 kWh/m^3). Biogas contains 50–70 vol% of CH_4, the most essential component from a calorific point of view. The other components, such as 2 vol% of H_2 and up to 45 vol% of CO_2, do not contribute to the energy in the combustion process and instead absorb energy from the combustion of CH_4 [5,6]. Biogas is utilized as a fuel for internal and external combustion engines that convert it to mechanical energy, which is then used to power an electric generator to generate electricity. The biogas yield of a plant also depends on the type of feedstock, fermentation conditions such as selection of bacteria, temperature, and hydraulic retention time. The calorific value of biogas is clearly the most important factor in an engine's performance.

The following technologies can be employed to convert biogas into electricity: a Stirling engine, a gas turbine, a micro gas turbine, high- or low- temperature fuel cells, a combination of a high-temperature fuel cell with a gas turbine, a spark-ignition engine, or a dual-fuel engine. Stirling engines (external combustion) are typically employed in specific applications and in concentrated solar power (CSP) plants. Internal combustion motors, whether gas or diesel, have become the standard technology and preferred solution for running biogas power plants today [7]. In Europe, 50% are spark-ignition internal combustion engine (ICEs) and about 50% are dual-fuel engines. Fuel cells and micro gas turbines are uncommon [8].

Hybridization solar and biomass technologies can provide sustainable energy services based on widely accessible indigenous resources, encourage sustainable development, and reduce reliance on a single renewable resource. Based on a series of thermodynamic, economic, and environmental evaluation outcomes, a hybrid solar-biomass system is recognized as a generally satisfactory mode [9,10].

Optimization of energy efficiency and environmental and/or economic performance is an important topic in such a hybrid system. A numerical model is used as a design method for analyzing the performance parameters of a microgrid power system in terms of economic, technical, and environmental considerations [11]. The results demonstrate a clear association between PV size and battery capacity. The battery bank capacity should be convenient to decrease the influence of the fuel cells (FC). The FC system also has an impact on the grid's resiliency. The correct sizing of the PV plant allows for more smart battery use and decreases dependency on grid electricity.

In northern Germany, the yields and optimization potential of 170 grid-connected PV installations were studied [12]. Using the annual in-plane irradiation and the actual peak powers of the PV modules and inverter particular efficiencies, the annual performance ratios have been determined to be in the range of 47.5–81% (mean of 66.5%). They are determined by inverter efficiencies, system design quality, and deviations between the listed module power rating and the actual peak power. The results indicate that comparing performance ratio values can assist in identifying factors that influence low final yields. The solar/hybrid/storage performance evaluation [13] provides an optimized energy yield estimation tool integrated with building geometry modeling to assess the possibilities of incorporating green energy into two Malaysian urban farm sites. The daily energy usage of vertical farms was 430.116 kWh and 1002.024 kWh. The research is aimed at the energy yield, performance ratio, economics, and environmental impact of solar/hybrid/storage for a vertical farming system. Grid-connected solar PV systems provided 11.6% and 8.35% of the load consumption in two sites, respectively. The key findings are that the performance ratios of grid-tied solar PV systems on both sites are 82.22% and 82.56%, respectively, and the systems have a lower levelised cost of energy (LCOE). On the other hand, the performance ratios of a standalone hybrid PV-battery-diesel system are 69.60% and 70.91%, respectively, and the systems' LCOE is the highest in all cases.

Much research has been conducted regarding the design and sizing of hybrid renewable energy systems. Several studies have focused on the system efficiency point of view and on the economic or environmental impact [14]. The optimum design of water-cooled hybrid thermoelectric power generator (CPV–TEG) systems [1] was determined using an overall performance index (OPI) that incorporates all performance indicators, energy efficiency, and costs of the hybrid system. The results indicate that when the direct normal irradiance DNI grows, the system's maximum energy efficiency decreases. Furthermore, the contribution of the thermoelectric power generator TEG does not work over a certain cell temperature.

Ma and others in [15] analyzed the long term performance of a standalone solar photovoltaic (SAPV) system with a capacity of 19.8 kWp. According to the results, the PV array functioned effectively, with an AC power generation efficiency of 10% and an overall system efficiency of 7.7%. The overall system yield is determined by the performance of the PV plant, inverters, and how well the battery bank and load match the solar source.

Furthermore, the temperature has an adverse impact on the power generation, especially during the summer months. The reference yield, array yield, and final yield are 4.08, 3.05, and 2.45 kWh/kWp/day, respectively; thus, the resultant performance ratio is 60%, indicating that the SAPV plant's performance during the reporting period was satisfactory. Environmental and operating data of a standalone PV system were collected over a two-year time period to examine its long term performance. The mismatch between the electricity production and the load consumption results from the energy utilization pattern of the local population on the island as well as the energy losses in the balance of system (BOS), inverters, battery bank, and conduction losses in the distribution cables. The results suggest that it would be better to develop or integrate the PV system into a microgrid.

The results shown by Bartolucci and others state that the correct sizing of the PV plant is a more affordable solution, where the battery is less reliant on the energy exchanged with the Electrical Main Grid (EG). A study [11] extended the work using the same performance indices where aspects such as economics, technology, and the environment have all also been considered. They conclude that the Network Operator's effects demonstrate how implementing a distributed energy conversion scenario via microgrids may benefit both prosumers and providers.

PV grid-connected performance depends on technical and ambient conditions such as cell technology, panel degradation inverters, wiring and configuration of installation, in addition to global irradiation, ambient temperature, and soiling losses.

Performance ratio (PR) is one of the main performance indicators and a simple tool used globally to broadly assess the overall plant performance. Several institutions, international projects, and experiments, such as NREL, the IEA PVPS Task Experiment, and the European Union participants' PERFORMANCE project, have employed PR as one of the major performance measures. They have provided different guidelines for evaluating the performance of PV systems, either for short–power (kW) or long-term energy (kWh) [16]. The ability to assess the performance of a stand-alone or grid connected PV system will assist in evaluating investments. Due to load matching and other unique operational features, the performance indices of grid connected, stand alone, and hybrid systems might change dramatically.

Temperature, low light, wiring, and inverter losses were among the several loss mechanisms identified in the simulation. Reich and co-workers reported for German climate conditions that a PR > 90% could not be achieved for mono-crystalline silicon reference cells [17]. However, it could be achievable today with commercially available components.

The objective of this work is to analyze the performance parameters of a hybrid (PV-BG) grid connected system located in Gaza city in terms of standard performance parameters such as yields, performance ratio, capacity factor, energy efficiency, and hourly energy output.

On the other hand, PVSYST software is a common piece of software used by designers of solar energy systems in this field [18]. It can provide the performance of the PV system, taking into account the losses through the system design, and provide the net performance ratio, e.g., PR is 76.1% of the grid-tied solar PV roof-top system for 364 kWp total capacity of the academic campus [19]. For a peak output of 48.12 kWp, the PR of a solar PV power plant is −87.2% [20].

Many reports in the literature have evaluated the techno-economic analysis designs, using the well-known HOMER software, for the grid-on or grid-off utility hybrid systems. HOMER provides optimized combinations of renewable and nonrenewable energy configuration components. The net present cost (NPC) and the levelized cost of energy are used to optimize and develop the system's size and components (LCOE). Work in [21] offers a performance analysis of a PV/Stirling battery system utilizing biomass in terms of energy efficiency, economic feasibility, and environmental sustainability. The system's performance is then compared to that of a hybrid PV/diesel/battery system. Both systems were sized using HOMER, a software tool for energy optimization, and MATLAB Simulink

TM 8.9, the latter being used to add dynamically for the performance system evaluation. The PV/Stirling battery combination proved to be a better performing choice for use in the electrification project, according to the results. A study [7] proposed the optimal sizing of biomass sharing for the autonomous or grid connected hybrid system depending on NPC and LCOE. The recommended configuration is PV/wind/diesel/biomass and is based on optimal solutions and cost analysis aspects. Furthermore, they also meet the electricity demand with additional (excess) electricity.

Depending on the literature review above and the various methodologies applied in system performance analysis. We provide a performance evaluating method for estimating the overall performance of the desired grid-tied, photovoltaic biomass configuration of the designed hybrid system. The contribution of our work is in offering a mathematical method for evaluating the performance of a hybrid renewable grid-connected system that depends on two types of renewable energy sources; solar energy and bioenergy. Energy harvests changes over the year based on the renewable energy resources (RES) shared in the hybrid system, which are various along the reported period time. To this aim, we have used the HOMER Pro program's hourly executed data as simulation results, which have been employed in the proposed calculating method to assess the effects of performance indicators on the regenerative hybrid system.

The paper has been structured as follows: Section 1 is an introduction, where the literature studies have been investigated with relation to the performance of systems that rely on solar energy and other resources. The suggested hybrid system for the research area has been also presented, including its configuration; In Section 2, performance parameters and indices of solar, biomass and others have been examined in detail; Section 3 displays the results employing the provided methodology; Finally, the conclusion in Section 4 describes the main outcomes and provides brief recommendations.

1.1. The Hybrid Power System Layout

The proposed hybrid system establishes a microgrid for the electrification of a residential district in Gaza, a Palestinian city center at an altitude of 49.7 m, latitude: 31°30′ N, longitude: 34°27′ E. The grid-tied hybrid system combines the energy derived from photovoltaic cells and biomass to feed a residential load exceeding 400,884 kWh annual AC primary load with a peak of 84.5 kWp and an average daily demand of roughly 1074 kWh/day. The NASA Surface Meteorology and Solar Energy webpage provided data on solar radiation [22]. In the winter, solar radiation is 2.87 kWh/m^2/day, whereas in the summer, it is 8.07 kWh/m^2/day. Agricultural waste, municipal solid waste (MSW), and sewage sludge (SS) are among the wastes used to generate biomass energy in Gaza. According to studies, solid waste has a high organic content of roughly 65%. This percentage is used to calculate the amount of waste that has been used and the amount of gas that has been produced by aerobic and anaerobic chemical decomposition. According to a 2017 survey, the average amount of waste produced per person per day is 1.05 kg [23].

The optimal capacity of the proposed HRE grid was obtained by HOMER Pro software consisting of a PV solar array of 150 kW capacity, 50 kW inverter, and two 25 and 70 (kW) biomass generators. The main components of the hybrid system as well as their different percent contributions to the electrical energy are shown in Table 1.

Table 1. Optimal component capacity configured by HOMER software.

Resources	Capacity Equipment (kW)	Electrical Energy (kWh/yr)	Percent (%)
Biomass	75	190,355	42.1
Grid	400	143,331	31.7
PV solar	150	118,468	26.2
Excess	-	46,119	10.2

Total electrical production of such a system is about 452,151 kWh/yr to cover the 400,884 kWh annual AC primary load. The annual energy produced by bio-generators is 190,355 kWh, which corresponds to about 42.1%.

The single-year results obtained from HOMER are taken as a reference for analyzing the hybrid system performance. The cycle charging strategy is considered in the proposed hybrid system.

1.2. Configuration of Hybrid Grid Tied System

A grid-connected system was designed for building a microgrid on the allocated area. The 150 kW PV system consists of 340 units of 440 W_p poly-crystalline PV modules with specifications under the standard test condition (STC) shown in Table 2. The performance, efficiency, and cost of the module, as well as the conditions in which it would operate, such as greater shading tolerance, should guide the selection of appropriate modules [24].

Table 2. CS3W440MS poly-crystalline module specification under STC.

Parameter	Specification
Maximum Power at STC (P_{max})	440 W
Optimum Operating Voltage (V_{mp})	40.7 V
Optimum Operating Current (I_{mp})	10.82 A
Open Circuit Voltage (V_{oc})	48.7 V
Short Circuit Current (I_{sc})	11.48 A
Module Efficiency	19.9%
Maximum System Voltage	1500 V (IEC/UL) or 1000 V (IEC/UL)
Power Tolerance	0 ~ +10 W
Dimensions	2108 × 1048 × 40 mm

The Sunny Tripower CORE1 grid-tie string topology inverters were used to interconnect the PV system [25], which are a three phase inverters of a maximum generator. The inverter specification data is shown in Table 3.

Table 3. Sunny Tripower CORE1 inverter specification.

Technical Data	Specification
75,000 Wp	75 kWp STC
Max. generator power	1000 V
MPP voltage range/rated input voltage	500 V to 800 V/670 V
Min. input voltage/start input voltage	150 V/188 V
Max. operating input current/per MPPT	120 A/20 A
Number of independent MPPT inputs/strings per MPP input	6/2
AC Rated power (at 230 V, 50 Hz)	50,000 W
AC nominal voltage	220 V/380 V 230 V/400 V 240 V/415 V
AC grid frequency/range	50 Hz/44 Hz to 55 Hz
Max. output current/rated output current	72.5 A/72.5 A
Output phases/AC connection	3/3-(N)-PE
Max. efficiency/European efficiency	98.3%/98.1%

The DC input power and AC output rated power are 75 kWp and 50 kW. The power output from the inverter is directly connected to the micro grid, and any excess energy is transferred to the utility grid. The choice of the inverter depends on its wattage, availability, price, reputation, and other considerations.

Many reports in the literature [24], for instance, use the temperature coefficient of the voltage to calculate the minimum and maximum operating voltage in the hottest and coldest site temperatures. Then, the number of PV modules in a string (N) ranges between minimum N_{min} and maximum N_{max} values. N_{min} is defined by the maximum power point (MPP) input DC voltage with regards to the V_{mpp} module. N_{max} is defined by the maximum input voltage of the inverter by the V_{oc} module. These values can be obtained in the module and inverter datasheet, as shown in Tables 2 and 3. This work uses the string technology inverter of six independent MPP inputs; both MPP entries have two strings (6/2) as depicted in Table 3. Then, the module number that can be connected in the series to make one string $\mathrm{N_{Module/string}}$ can be found according to the maximum DC power of the inverter (50 kW), number of strings (6 × 2), and maximum power of the model (P_{max}) and calculated by the following equation:

$$\mathrm{N_{Module/string}} = \frac{\mathrm{P_{DC,Max,inverter}}}{12 \times \mathrm{P_{DC,Max,module}}} \tag{1}$$

A 14 module/string was selected that can satisfy the inverter capacity of 75 kW and (14 × 48.7 = 681.8 V), which is less than the maximum system voltage (1000 V DC). Hence, building a 150 kW PV system capacity in the desired hybrid system required three PV subarrays with a capacity of (14 × 12 × 440 W) 73,920 kW_p, each implemented by a 50 kW inverter. Appropriate wiring/cable for the electrical connection should be used to minimize the voltage drop and power losses in the cables. Losses due to the cables are defined by many factors: cable length, operating voltage and current, operating temperature, and allowed potential voltage drop [19].

2. Methodology

2.1. Performance Parameters and Indices

Parameter indices are used to analyze the results achieved on an hourly basis over the duration of a project year. Firstly, the main assumption for evaluating the performance parameters is presented and then the numerical results are analyzed. The derived energy quantities are measured in real time according to IEC 61724 and defined by the following equation:

$$\mathrm{E_{i,r}} = \tau_\mathrm{r} \times \sum\nolimits_{\tau} \mathrm{P_i} \tag{2}$$

where the energy (kWh) is equal to the sum of the power (kW) parameter across the reporting time period for the recording interval τ_r. Both τ_r and τ are measured in (h). By using this formula, various net energy quantities are defined. In such a system, the energy is delivered from a PV array, a bio-generator, and from the utility grid implemented. Figure 1 depicts the input and output energies, with values calculated using Equations (1)–(6).

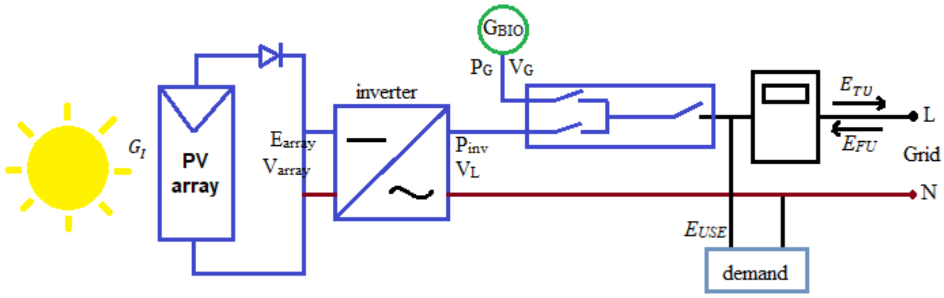

Figure 1. Parameters of the desired hybrid system to be measured in real time.

In the same manner, mean daily irradiation quantities $H_{I,d}$ are evaluated from the recorded irradiance in the plane of the array G_I using the following equation.

$$H_{I,d} = 24 \times \tau_r \times \left(\sum\nolimits_{\tau} G_I\right) / \left(\sum\nolimits_{\tau} \tau_{MA} 1000\right) \tag{3}$$

τ_{MA} (h) is the availability of the monitored data in the reporting time period τ (h).

The net energy delivered to the utility grid in the reporting period τ is

$$E_{TUN,\tau} = E_{TU,\tau} - E_{FU,\tau} \tag{4}$$

The net energy delivered from the utility grid in the reporting period τ is

$$E_{FUN,\tau} = E_{FU,\tau} - E_{TU,\tau} \tag{5}$$

The total system input energy is

$$E_{in,\tau} = E_{A,\tau} + E_{BG,\tau} + E_{FUN,\tau} \tag{6}$$

where A stands for the array, $E_{A,\tau}$ is the amount of energy affected by solar radiation and module temperature, and BG indicates the biogas unit. In this work, the hourly energy production is evaluated over a single year by HOMER Pro

The total system output energy is

$$E_{USE,\tau} = E_{L,\tau} + E_{TUN,\tau} \tag{7}$$

where L stands for load and U stands for utility grid.

The fraction of the PV array energy with regard to all sources is

$$F_{A,\tau} = E_{A,\tau} / E_{in,\tau} \tag{8}$$

The efficiency with which the energy from all sources is transferred and consumed by the loads is

$$\eta_{LOAD} = E_{USE,\tau} / E_{in,\tau} \tag{9}$$

The overall efficiency of the BOS components is calculated by the following equation: [26]

$$\eta_{BOS} = \left(E_{L,\tau} + E_{TUN,\tau} - E_{FUN,\tau}\right) / \left(E_{A,\tau} + E_{BG,\tau}\right) \tag{10}$$

The inverter's rating has been determined based on the peak load demand using Equation (11) and is 50 kW, with a 95% efficiency as described in HOMER. The Sunny Tripower CORE1 inverter's instantaneous efficiency may be measured by dividing the inverter output power by the PV power, which equals the PV current I_{PV} multiplied by the PV voltage V_{PV} using the formula.

$$\eta_{SMCinv} = \frac{P_{SMC}}{V_{PV} \times I_{PV}} \times 100\% \tag{11}$$

2.2. PV Performance Indices

The International Electro-technical Commission (IEC) provided a mathematical description of the PV system's electrical output as a function of meteorological conditions, system components, and system design. Parameters such as "performance ratio" and "performance index" are defined in the new IEC 61724 "Photovoltaic system performance" series of standards. The grid-connected PV system performance is computed depending to several parameters: energy production of the PV system (E_{DC}), PV yields: array yield (Y_a), final yield (Y_f), reference yield (Y_r), performance ratio (PR), capacity factor (CF), energy efficiency, and system losses. The PV performance indicators can tell us how well a PV system is performing in terms of the amount of energy it produces in a given amount of time as well as the amount of irradiation it receives.

The array yield (Y_a) is measured in kWh/kWp and is calculated by dividing the amount of DC energy delivered by the PV system's nominal power. It represents the time (hourly) that the PV system must be operating with its nominal power to meet the defined energy demand

$$Y_a = \frac{E_{DC}}{P_{pv,\ rated}} = \tau_r \times \left(\sum_{day} P_A\right) / P_{pv,\ rated} \tag{12}$$

where E_{DC} is a hourly total DC energy delivered by the PV system (kWh) and $P_{pv,\ rated}$ is the nominal power of the PV system (kWp). $\sum_{day} P_A$ is the actual power generated by the PV array in the monitored interval τ_r.

The final yield of the PV plant (Y_f) is measured in kWh/kW$_p$ and is defined as the ratio of the total AC energy delivered by the PV system during a specific period to the nominal power of the installed PV system. It indicates how many hours a day the PV system must run at its nominal power $P_{pv,rated}$ in order to match its monitored contribution to the net daily load.

$$Y_f = \frac{E_{AC}}{P_{pv,rated}} \tag{13}$$

$$Y_f = Y_a \times \eta_{pv,sys} \tag{14}$$

Efficiency of the PV system is $\eta_{pv,sys}$.

The reference yield (Y_r) is measured in kWh/kWp and is calculated by comparing the global solar radiation of the desired location to the reference irradiance ($G_{I,ref}$) of the PV system. The value of $G_{I,ref}$ is 1 kW/m^2 at the standard test condition (STC). Y_r is called the peak sun hour (PSH). The reference yield is the amount of theoretical energy available at a given site over a given time period. It represents the same energy that was actually monitored.

$$Y_r = \tau_r \times \left(\sum_{day} G_I\right) / G_{I,ref} \tag{15}$$

Based on the system name-plate rating, the PR is the ratio of measured output to expected output for a specific reporting period. It is an indicator of the overall influence on the PV system's rated output. International Electro Technical Commission's standard IEC 61724 [26] and other widely used key reference documents for the monitoring of a PV plant, such as NREL, IEAPVPSTask2, European Guidelines, and Australian PV System Monitoring Guideline, all report PR as the ratio of the final system yield (Y_f) to that of the reference yield (Y_r). It indicates the overall effect of losses on the plant's rated array output due to ambient conditions such as temperature, irradiation, as well as system component inefficiencies like the inverter, cabling, connections, or failure, etc.

$$\text{Performance Ratio (PR)} = \frac{Y_f}{Y_r} \tag{16}$$

PR can be determined by using the simplified formula rather than using the normalized parameter

$$PR = \frac{E_{actual}}{E_{nominal}} \tag{17}$$

where E_{actual} is the actual PV plant energy generated and consumed by the load side at the end of the analysis period, $E_{nominal}$ is the calculated nominal PV plant output, which is equal to the total solar radiation incident on the entire module surface multiplied by the PV module nominal efficiency at standard conditions (STC).

The array capture losses (L_C) are caused by the losses on the PV array, whereas the (L_s) PV losses are caused by the inverter's DC–AC conversion. The BOS losses (L_{BOS}) can be calculated using the following equations:

$$L_c = Y_r - Y_a \tag{18}$$

$$L_s = Y_a - Y_f \tag{19}$$

$$L_{BOS} = Y_a \times (1 - \eta_{BOS}) \quad (20)$$

It is worth noting that the IEC 61724 recommends utilizing multiple criteria and limitations for distinct metrics in the monitoring approach.

The PV system includes PV arrays and inverters, and the efficiency of the system can be defined as the ratio of the AC-energy generated to the mean daily irradiation quantities $H_{I,d}$. These are calculated using the actual irradiance in the array's plane.

$$\eta_{pv,sys} = \frac{E_{AC}}{H_{I,d}} \times 100\% \quad (21)$$

On the other hand, the immediate solar PV module conversion efficiency is computed by

$$\eta_{PV} = \frac{E_A}{A \cdot \int G_t dt} \times 100\% \quad (22)$$

where η_{PV} is the immediate conversion efficiency, G_t is the incident solar radiation per unit area of the tilted PV panel (W/m^2), A is the total solar cell area (m^2), and t is the time period, during which the solar radiation exists (h).

The capacity factor depicts the PV plant's efficiency. It is the ratio of real power created to theoretical power; for example, the capacity factor for one year is equal to the real (average) power generated (kWh/year) to the nominal power generated (kW) $\times$ 8760 h/yr. When calculating *CF*, it is recommended that the AC voltage values are utilized.

$$CF = \frac{P_{avg}}{P_{pv,rated}} \quad (23)$$

2.3. Biomass Generator

In [27], the biomass available in the study area is waste biomass, which includes municipal waste, agriculture residue, and sewage sludge. The biomass energy source is suitable for producing electricity and can cover, with solar PV panels, 60% of the residential electrification. Depending on the biomass characteristic and the conversion technologies requirements for different technologies, anaerobic digestion has been selected to provide electricity.

Biogas produced in such a conversion is finally supplied to the biogas internal combustion engine (ICE) to generate electricity. ICE has a higher power generation efficiency, usually between 30% and 45%, compared to ordinary gas turbine and steam turbine systems. Biogas engines can work with low-caloric gaseous fuels and low gas pressures. The power supply range of a single-machine ICE is between 1 kW to 4 MW. Therefore, the ICEs can be operated on full load or partial load, both with high efficiencies [28].

Figure 2 shows the monthly available average biomass potential broken down on a daily average (tons/day). The annual average potential of biomass as feedstock to the AD plant in the test area is 719.25 t/d. The average price (USD/ton) of biomass is defined as two values, 40 and 100. The carbon content in the feedstock and AD conversion efficiency are defined to be 50% and 0.9 (kg/kg), respectively.

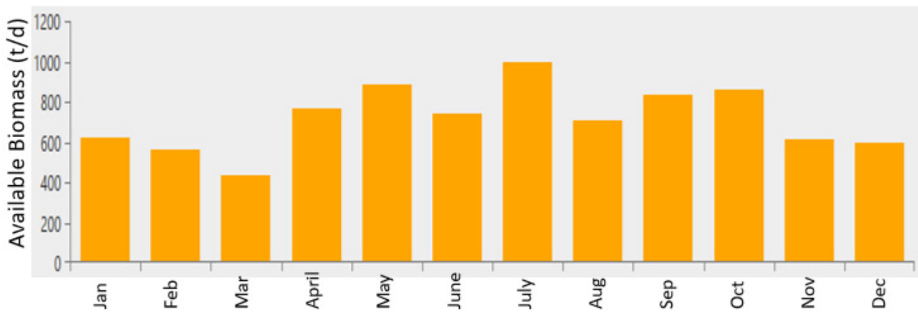

Figure 2. Daily available biomass over a year (tons/day).

Biogas is composed of different gases and substances, namely methane (CH_4), propane (C_3H_8), carbon dioxide (CO_2), and nitrogen (N_2). This study assumes 60% CH_4, 38% CO_2, and 2% others. The physiochemical properties of biogas are displayed in Table 4. Biogas has an average calorific value of 21–23.5 MJ/m^3, which means that 1 m^3 of biogas is equivalent to 0.5–0.6 L of diesel fuel or roughly 6 kWh [29].

Table 4. Physicochemical properties of biogases.

Parameter	Unit	Value
Lower heating value (LHV)	MJ/m^3	20
Higher heating value (HHV)	MJ/m^3	29.5
Specific fuel consumption	kg/kWh	1.23
Density	kg/m^3	0.817

ICE is used to generate power in the plant. The overall biogas system efficiency to produce electricity can be determined from the following equation.

$$\eta_{elec} = {}^{P_{net}}/\dot{m} * LHV \tag{24}$$

where P_{net} (kW) presents the effective amount of electrical and auxiliary power being generated. The auxiliary power is needed for different electrical components, including compressors, pumps, etc. The fuel flow is $\dot{m}$ (kg/s) and the lower heating value is LHV (MJ/kg).

Biogas is a crucial component of the hybrid system that has been defined. Waste biomass, as well as organic residues, were chosen to contribute to the production of electricity in the residential district of the microgrid network for environmental and economic sustainability considerations, as well as for social reasons. Biomass resource data employed for the microgrid are shown in Table 4. The proposed hybrid system includes two biogas engines with 25 kW and 50 kW capacity.

2.4. Class Index (I_{size})

Several indices are typically used to define the efficiency of a micro grid based on renewable energy. The first one is the so called class index I_{size}, which represents the ratio of the overall energy demand over the potential energy that can be generated by renewable energy sources (RES), and is stated as follows [30]:

$$I_{size} = \frac{E_{load}}{E_{RES}} \tag{25}$$

2.5. Self-Consumption Index

The renewable energy systems seek the highest consumption and benefit from the renewable energy produced in the microgrid, which reduces the losses and costs of such a grid. The self-consumption index [11] is defined as the ratio of the energy locally consumed from RES to the total energy produced by RES.

$$I_{consumption} = \frac{E_{RES} - E_{sold}}{E_{RES}} \tag{26}$$

2.6. Economic Indices

The proposed hybrid system was selected based on the techno-economic feasibility that achieves an affordable optimal solution. Many important economic values have been provided by HOMER Pro, including economical values of the components: capital cost (CC), operating and maintenance costs (O&M), and replacement cost. Other economic values are considered, such as grid utility energy cost (USD/kWh) and the fuel price. In the desired hybrid system, the fuel cost includes the average cost of the biomass required (USD/ton) and hourly operating cost (USD) for the biogas generators. Achieving energy system affordability is based on using a more economical source of energy as well as efficiency improvements. The cost of energy supplied by the grid for a residential application is 0.143 USD/kWh.

2.6.1. Discount and Inflation Rate

The values of 10% and 4% were chosen and implemented into HOMER as the nominal discount and expected inflation rates to satisfy the winner solution. These values obviously influence the economy and could be subject to a parameter variation and sensitivity analysis. However, the chosen values represent actual numbers for the selected model region.

2.6.2. Hybrid System Component Cost

Component cost involves capital cost (CC), operating and maintenance (O&M) costs, and replacement cost. They all were assumed to be fixed values that were inserted before a simulation run.

2.6.3. Payback Period (PBP)

By comparing one system to another, HOMER determines payback. Payback is a term that describes how long it takes to recover an investment. A particular amount of money is originally invested, and subsequently revenue is generated from it. The payback period is defined as the number of years it takes for the total income to match the initial investment. One of the two systems compared is the winner system, which is named the proposed system. The other one is named the base system, which should be chosen from the list of optimization results. When conducting a comparison between the winner system with the base system, it is determined that the simple payback is 0.04 years. Only when we compare one system to another does the concept of payback make sense; hence, we have to define the base system that will be the proposed hybrid renewable system instead. The designer constantly uses a non-renewable power system as the base case, however HOMER permits any base case to be specified; for example, to calculate the payback of the biogas engine, a system with a PV array was compared to a system with a PV array, plus a biogas engine.

2.7. Environmental Data Assessment

The operating performance of a renewable system is highly dependent on the local environmental conditions such as solar radiation, ambient temperature, wind speed, and dust storms [31]. The average daily global solar radiation on a horizontal surface for each month of the year is shown in Figure 3. The average daily total values range from 2.870 kWh/m^2/day in December to 8.070 kW h/m^2/day in June. The yearly average value is 5.57 kWh/m^2/day.

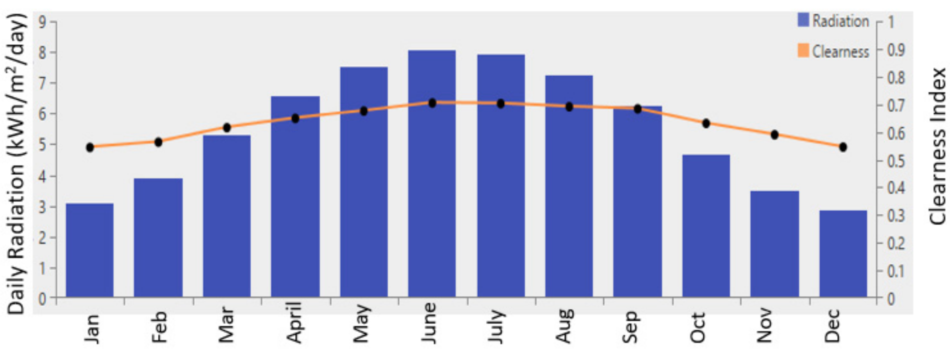

Figure 3. Monthly average for global horizontal radiation in kWh/m^2/day, over a 22-year period (Jul. 1983–Jun. 2005), Homer Pro.

Figure 4 shows the monthly mean temperatures of ambient air over one year based on data from 1984 until 2013. The ambient temperature of the PV system varied from 15.22 °C in February and 26.86 °C in August, and the annual average temperature is 20.99 °C. While the temperature of the PV modules varied substantially from 30 °C to 60 °C, temperature effects are not implemented into this study.

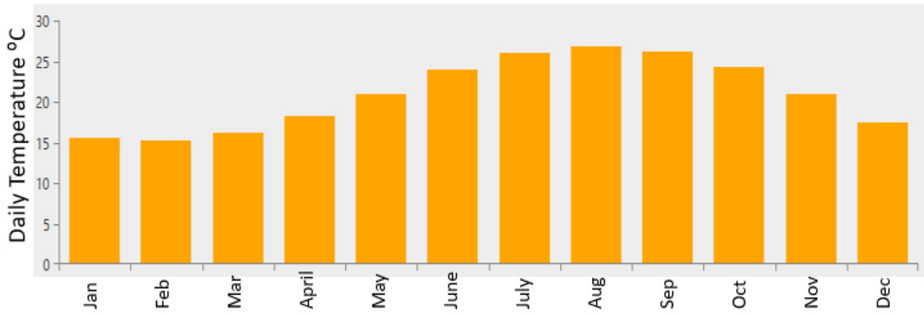

Figure 4. Monthly average air temperature (°C) over a 30-years period (Jan. 1984–Dec. 2013), HOMER Pro.

3. Results Analysis

The experimental results were obtained from conducted simulation runs with HOMER Pro. The results involve values for generated electricity by the various components, as well as electricity purchased from the utility grid. It also includes the electricity consumed by primary AC loads, the resold electricity, fuel rates, solar radiation and finally the percentage and the penetration of renewable energy of the whole system. The results were employed to analyze the hybrid system performance for the selected location with an averaged global solar radiation of 5.57 kWh/m^2/day, an annual mean temperature of 20.27 °C, and a biomass price of USD40/ton. The combined PV-biogas generator grid connected hybrid power system is found to be the option that offers the most economically effective solution, option based on the net present cost (NPC) and the cost of electricity (COE).

The renewable energy contribution to the corresponding energy system is 64.3% with a maximum renewable penetration of 497%. A hybrid power system capacity with a 400 kW utility grid comprises of 150 kW solar PV, 75 kW bio generator(s), and 50 kW converter to meet the required electrical load, and the excess electricity of 46,332 kWh (10%) can be used to serve the future prolonged demand or any unanticipated additional electrical load. Table 5 also shows that the combined contribution of energy generated by biomass resources utilizing bio-generators and PV accounts for 42.4% electricity generated by the hybrid power system.

Table 5. Electricity generated and consumed by the power system components.

Production	kWh/yr	%	Consumption	kWh/yr	%
Generic flat plate PV	118,623	26.2	AC primary Electrical load	400,884	99.7
Generic 25 kW bio-generator	56,819	12.6	DC primary Electrical load	0	0
Generic 50 kW bio-generator	133,266	29.8	Deferrable load	0	0
Grid purchases	143,443	31.7	Grid sales	1203	0.299
Total	452,151	100	Total	402,087	100

In general, it can be reported that a high proportion of the renewable energy contribution of the total electricity produced in the hybrid system can reduce the dependence on diesel price, lower the operating and maintenance, as well as lower fuel costs, even though it is a challenge to control the system and maintain a stable voltage and frequency, which is an issue related to the intermittent nature of renewable resources over time, and presents a challenge. The 64.3% contribution of the PV system and biomass engines of the total energy generated by the hybrid power system observed in this study are a good compromise for the interested area that possesses abundant renewable energy resources, but has high diesel prices [32].

The monthly average of electricity produced by each power generating unit of the hybrid power plant is presented in Figure 5. The figure indicates that electricity produced by each component varies from one component to another and from month to month. This is mainly due to the variability in monthly global solar radiation, mean biomass quantity and quality, and the limited availability of the utility grid. In November, the PV and bio-generators generated an average monthly power of 18.75 kW, with a maximum power production of 140.3 kW. In September, the bio-generators generate power ranging from 18.75 kW (lowest renewable energy conversion) to 75 kW.

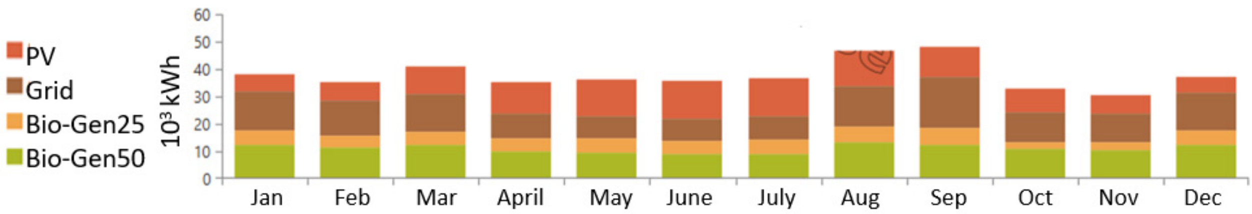

Figure 5. Monthly distribution of the hybrid energy system's average power generation.

Based on the performance model procedures in Section 3 and the hourly executed data of a single-year as simulated with the software, the performance of individual components of the hybrid system, as well as the entire system, has been investigated using HOMER Pro. Furthermore, the PV system performance has been assessed with respect to the inverters. The relationship between the PV component performance and the irradiation has been explored as well. Finally, the energy performance of the overall system was analyzed in terms of normalized parameters, performance ratios, production factors, and energy balances. The global solar irradiation, as well as the incident solar spectrum, are shown in Figure 6 during the sunshine hours for January and June. The peak value is different in the two curves; in the summer semester, it occurs at noon.

The PV electric power generated from global incident radiation for the 31st of January and 31st June are shown in Figure 7. The power generated from 4 am to 11 am in the morning (red line) increases and then decreases from 12 pm to 5 pm in the afternoon. The power output versus the solar radiation is shown for the 31st of June in Figure 7.

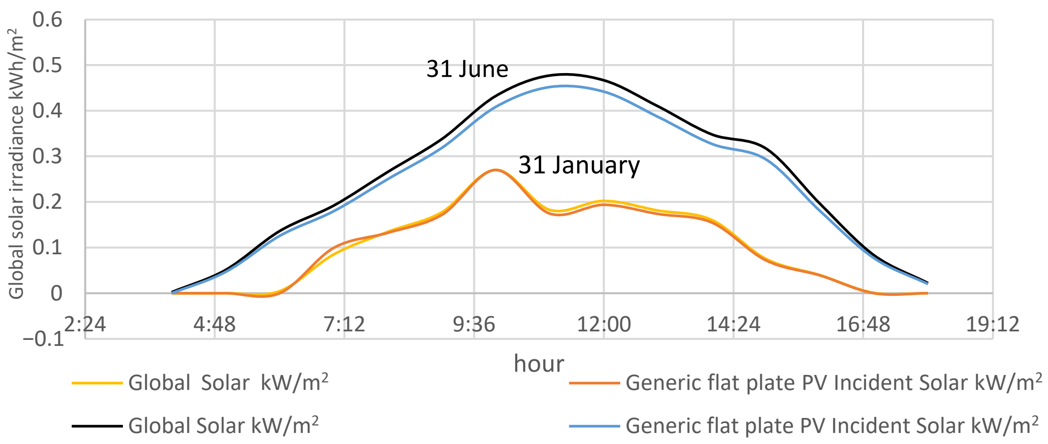

Figure 6. Global solar irradiance curve for two days, 30 June and 31 January (2007).

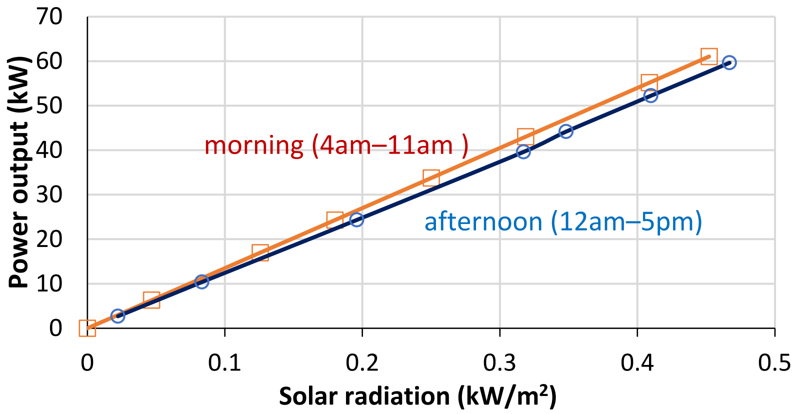

Figure 7. Electricity production (kW) by the PV array system on 31 June.

The immediate conversion efficiency of the module system may be calculated using the power output produced by the PV array and the solar radiation intensity, as shown in Equation (22), as an example, in the first week of January 2007. It turned out, as depicted in Figure 8, that the PV efficiency is 41%, which has finally been set for the simulations with HOMER. The efficiency is defined as the ratio of the PV output module power (before entering the inverter) to the incident radiation power. The chosen efficiency is higher than that scored by STC as it is calculated with respect to the solar incident radiation and is using the maximum power value achieved in a hybrid system of 150 kW. Thus, 65.3 kW could be provided on average. The efficiency of the inverter has been set at 95% according to Equation (10).

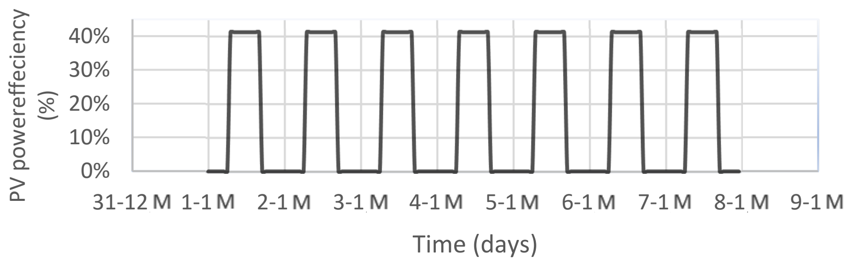

Figure 8. DC power efficiency (%) of the PV array for the first week of January.

The electrical efficiency of the biomass unit has been evaluated using Equation (24), which considers the output electric power of two bio-generators (25 kW, 50 kW), that are created according to the biomass fuel flow and LHV. From the simulated results, it is determined that the efficiency is around 50%, as shown in Figure 9. Zero values of efficiency scores happen at the force-off operating mode indication in the bio-generator scheduler operation, that is inserted to the simulation process, while the electric power can be generated by other production components. As an input, the fuel consumption of both bio-generators (25, 50 kW) is set to 32.21 and 60 kg/h, respectively, and these values obviously vary throughout the operating year. Finally, the specific fuel consumption is 1.26 kg/kWh.

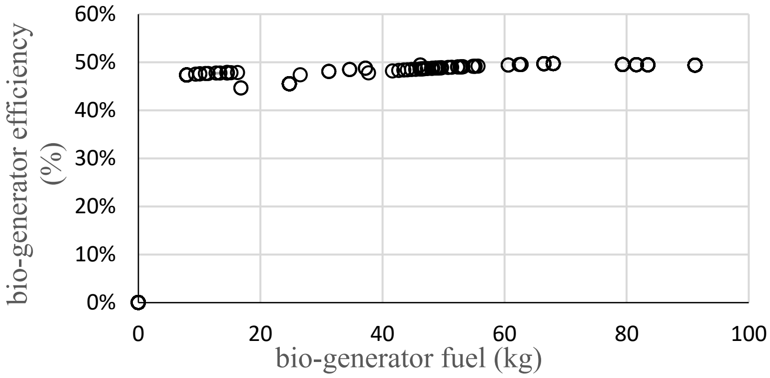

Figure 9. Biomass system efficiency (%) with respect to fuel mass (kg).

In the whole system, the performance of the electricity generation and load consumption over the reporting period, which is hourly data for one year, are presented. PV plants, bio-generators, and grid-purchased electricity generate the electricity, which is consumed by the AC electric load and utility sales. During a year of operation, the 150 kWp PV system generates a total electricity of 118,623 kWh and the average daily production is 325 kWh. The annual electrical production of the two 25 and 50 kW bio-generators are 56,819 kWh/yr and 133,266 kWh/yr; hence, the daily production is 157.8 kWh and 370.2 kWh. The annual grid energy purchase is 143,443 kWh, which is distributed among the months, as shown in Table 6, with an average daily purchase of 597.68 kWh. The table shows the monthly energy sold (kWh), energy purchased (kWh), and corresponding peak load (kW). Energy generated from hybrid components is consumed by the AC primary load that equals 400,884 kWh/yr, and the annual grid energy sold is only 1203 kWh. The hourly energy production and consumption data for two representative days in January and August are presented in Figure 10. It is clear that there was some mismatch between the energy supply and demand in the system during the daytime in January; production is more than consumption. In August, it is obvious that load-side consumption converges with production time distribution. This is owing to the fact that the load profile in the summer season differs from the load profile in the winter season. Excess electricity is defined as surplus electricity.

Table 6. Monthly electrical energy purchases and sales by the utility grid and corresponding peak load.

Month	Energy Purchased (kWh)	Energy Sold (kWh)	Net Energy Purchased (kWh)	Peak Load (kW)
January	14,468	0	14,468	84
February	12,707	0	12,707	84
March	13,751	0	13,751	84
April	9149	0	9194	82
May	8540	0	8540	79
June	7978	0	7978	78
July	8238	0	8238	79
August	14,716	352	14,364	79
September	18,466	444	18,022	81
October	10,660	168	10,492	81
November	10,581	221	10,360	59
December	14,144	19	14,125	84
Annual	143,443	1203	142,239	84

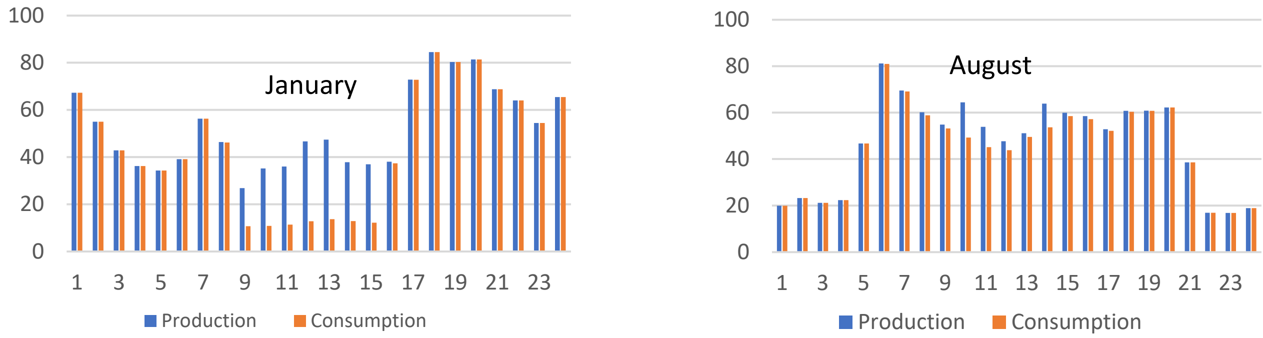

(**a**) (**b**)

Figure 10. Daily average electricity production and load consumption over the reporting period, January (**a**) and August (**b**).

The energy losses in the BOS cause the difference between the power generation and consumption, including the PV equipment, cable losses, and biomass generation losses. Figure 11 depicts the relation between production and consumption with a linear slope of approximately one in January (Figure 11a) and 0.972 in August (Figure 11b). The normalized parameter usage factor (UF) is equivalent to the slope of the fitting line at 1.03 and 0.972 in both months, which is expressed as the overall efficiency of BOS. The results reveal a high performance of the whole system that HOMER Pro seeks to use for an optimal and affordable solution with the best combinations of the electrical components.

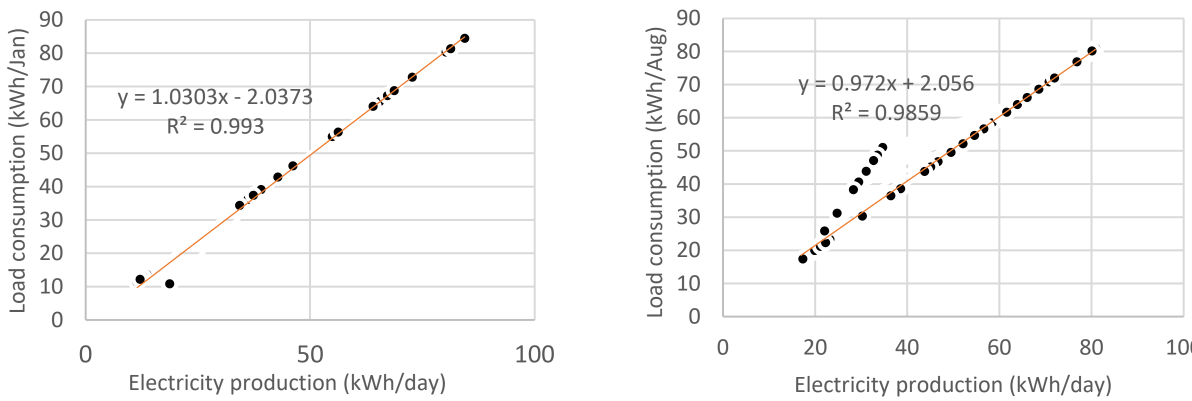

(**a**) (**b**)

Figure 11. The monthly average power consumption and production correlation, January (**a**) and August (**b**).

To increase the energy utilization from biomass components, the specific fuel consumption (kg/kWh) should satisfy the case in which the calorific value of the biomass is used to generate energy. Four typical seasonal days of winter, spring, summer, autumn, for example, 11 January, 11 May, 11 June, and 11 October, which are characterized on the basis of the daily average solar irradiation from 6:00 to 18:00, are used to examine the detailed electricity generation and consumption on different days, as illustrated in Figure 12.

In the case of 11 May and 11 June, the average solar irradiation between 6:00 and 18:00 was about 7.500 kWh/m^2/day and 8.070 kWh/m^2/day, and therefore, the PV array's energy production was the highest of the renewable fraction. The average irradiation in October is 4670 kWh/m^2/day and the consumption rate is relatively low. Grid purchased electricity is the highest in January, while the biomass bio-generators are stable with regard to the production and the consumption rate over four seasons.

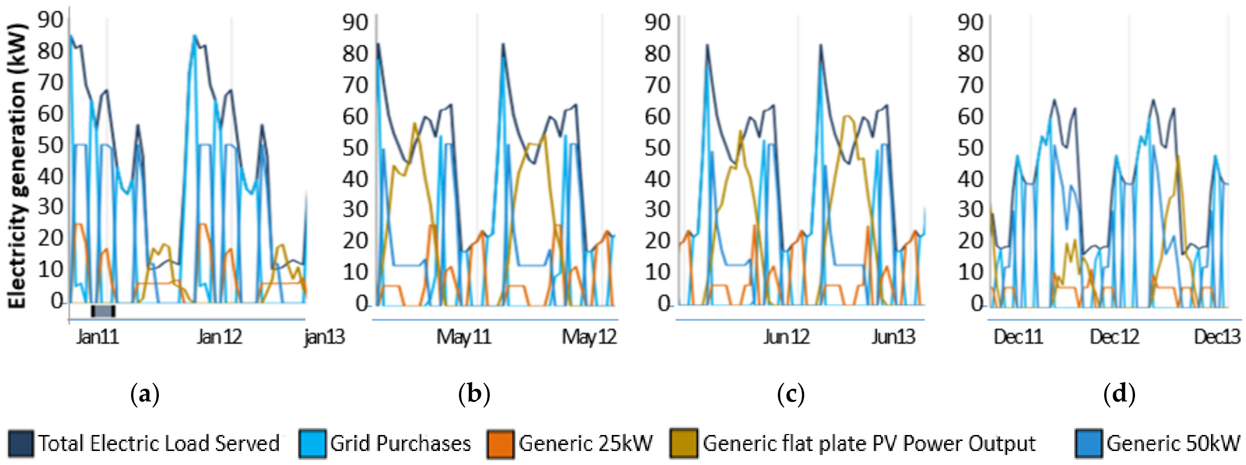

Figure 12. Electricity generation (Grid, PV, and biomass generic 25 kW, 50 kW) and total electrical load served on 11 January (**a**), 11 May (**b**), 11 June (**c**), and 11 October 2007 (**d**).

Based on the calculation model provided in Section 3 that emanate from IEC 61724, the normalized performance characteristics of the PV system in the hybrid system are investigated. Figure 13 presents the daily performance ratio parameter results during the reporting period of two months, January and June of the year 2007.

The specific indicator, performance ratio (PR), is found by evaluating the ratio between two normalized performance parameters, the final yield to reference yield, according to Equation (16). In this work, it is evaluated by using the simplified formula in Equation (17) that defines the PR as a ratio of the real PV energy vs. the nominal PV energy. The output AC power of the inverter of the hourly single-year data is substituted as the actual energy of the PV. The nominal energy is calculated by multiplying the hourly incident solar radiation by the panel area that covers the PV system's maximum power output, which equals 65.3 kW for the intended hybrid system. The dimensions of the 440 W PV module are given in Table 2. Figure 13 shows the PR for January and June in the daytime. It is obvious that the PR does not reach 40% in both months; in January, many scored values remain in the range of 5–10%. When the inverter output is zero, notwithstanding incident radiation, this is termed as a zero value. In June, the PR for such a system was estimated to be between 20% and 40%. June has higher score values than January due to two more daily sunshine hours.

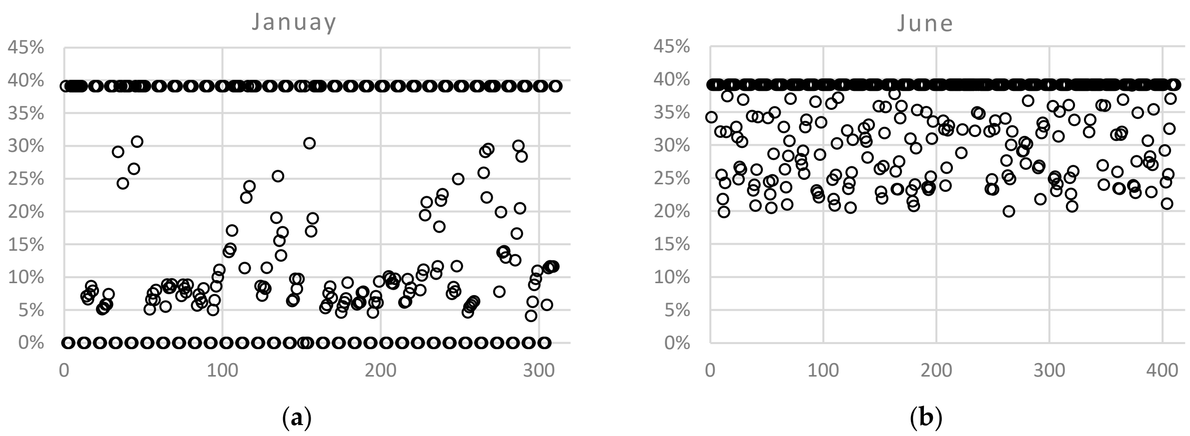

Figure 13. The PV-grid connected hybrid system's PR in January (**a**) and June (**b**).

A higher performance ratio indicates more utilization of energy. A PR of 20% indicates that 80% of the expected production from incident solar radiation is either not transformed into usable energy or is not utilized by the load. This is due to low incident radiation relative to the inverter's operating point, as well as the dependency of the system on other energy sources. The PR in Switzerland and the Netherlands is 0.69, followed by 0.67 in Germany and 0.43 in Italy, according to data from 140 PV systems in IEA countries [33].

In the same context, the capacity factor varies throughout the year. In January and June, hourly data from two distinct months have been utilized to compute the capacity factor. Using Equation (23), the CF is found to vary seasonally, as shown in Figure 14. In January, a low capacity factor of less than 16% occurred for about a third of the recorded data in this month's readings (Figure 14a), where the CF did not exceed 80%. The readings involve values during the daytime. The reporting data is higher in June due to more sun hours in the summer, and the CF is high as well (over 80%), which represents a quarter of the population, as seen in Figure 14b. According to the literature, solar PV plants' capacity factors range from 15 to 25%, while PV cells with a 45% efficiency have been manufactured.

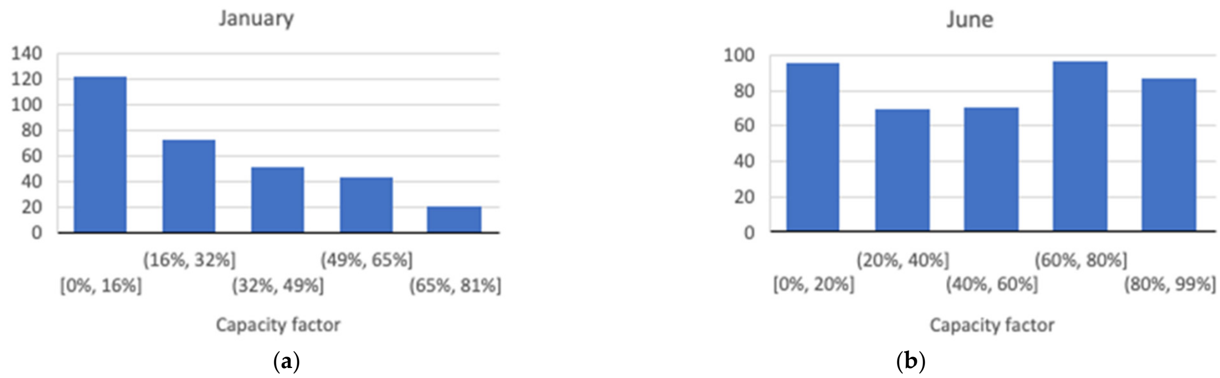

Figure 14. Capacity factor repetitions for the PV system in a hybrid system.

This work reports average yields from the PV units recorded in January: Y_a, Y_f, and Y_r of 5.76 kWh/kWp/d, 1.44 kWh/kWp/d, and 3.08 kWh/kWp/d, respectively. A study [34] of a 10.6 kWp grid-tied PV system within the eight-month monitored period reported a performance ratio average value and capacity factor of 82.42% and 14.07%, respectively, with average yield values: array, final, and reference of 3.49 kWh/kWp/d, 3.38 kWh/kWp/d, and 4.12 kWh/kWp/d, respectively.

Renewable penetration (RP) is calculated in every step time by HOMER. It is calculated by dividing the total renewable electrical power (kW) production of the hybrid system by the total electrical load served (kW) in a given time step. The maximum renewable penetration reported by HOMER is 497%, which obviously occurred in January, where the bio and solar renewable resources have served the load in its low values. The solar produced in winter is unexpected due to the cloudy and colder climate. This led to high renewable penetration as shown in Figure 15a. In July, the maximum RP was reported to be around 150%. Not only does the abundant solar radiation decrease this value, the load profile that nearly matches the renewable resources does as well, as shown in Figure 15b. In both months, RS exceeds the demand power, which leads to an RP that is more than one hundred percent; this is what the simulation is aiming towards. On the other hand, zero renewable penetration scored at night time, when the system was depending on the grid. In the same context, class index, as described in Equation (25), is practically the inverse value of the RP; both class index and RP are inverse multiplication. Figure 16 depicts the relation between overall energy consumption and potential energy produced by renewable energy sources. The ratio is known as the class index, as depicted in Figure 17. There is a match between the served load and the renewable resources for both months. In some cases, the renewable energy produced varies, although it is still below the load served, and grid purchase covers the load in such cases where the renewable fraction is below 100%.

The self-consumption index used by Equation (26), or excess renewable energy generated by the desired system or renewable resources consumption, is another useful index. The index is useful for excess energy control and the issue of trade off economic adaptation, with very small values of that index indicating a small energy sellback to the grid and low excess electricity produced from renewable resources. As no renewable energy is generated or therefore sold, undefined values of the index are remarked as being zero values, as shown in Figure 17. HOMER calculates the grid sales (1203 kWh/yr) that are comparable to 0.299% of the annual energy consumption of 402,087 kWh/yr.

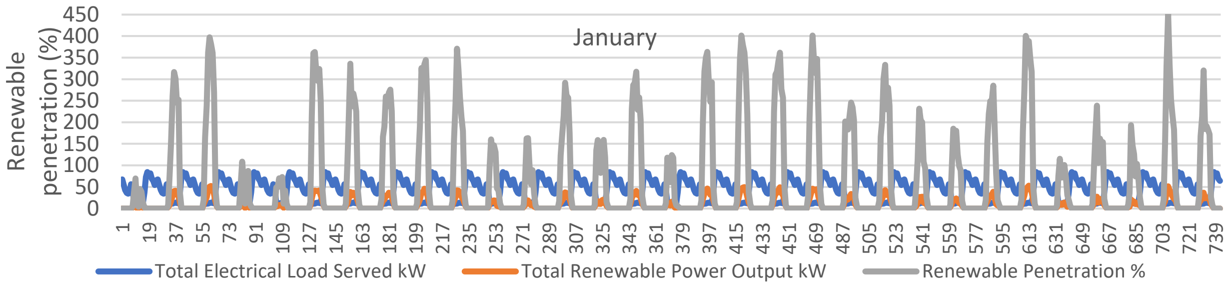

(**a**)

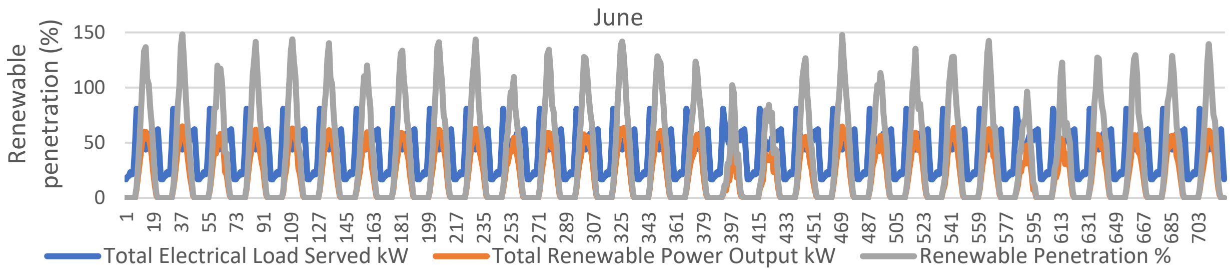

(**b**)

Figure 15. Renewable penetration values (%) scored in January (**a**) and June (**b**).

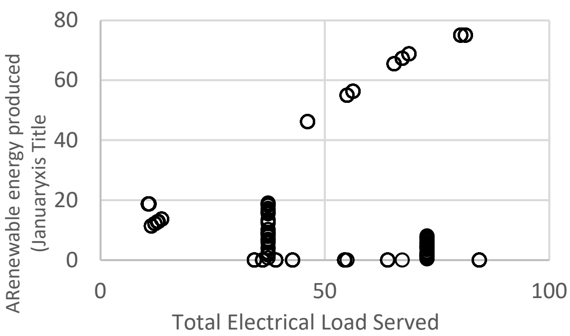

(**a**)

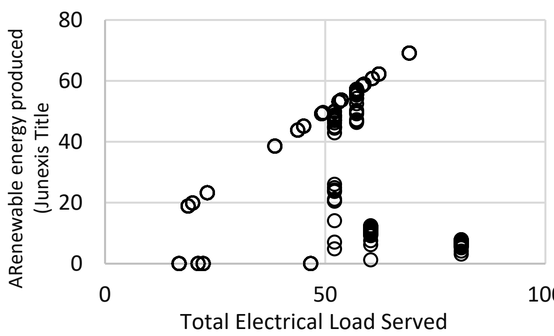

(**b**)

Figure 16. Class index; the potential renewable energy (kW) that served the total energy demand (kW), January (**a**), June (**b**).

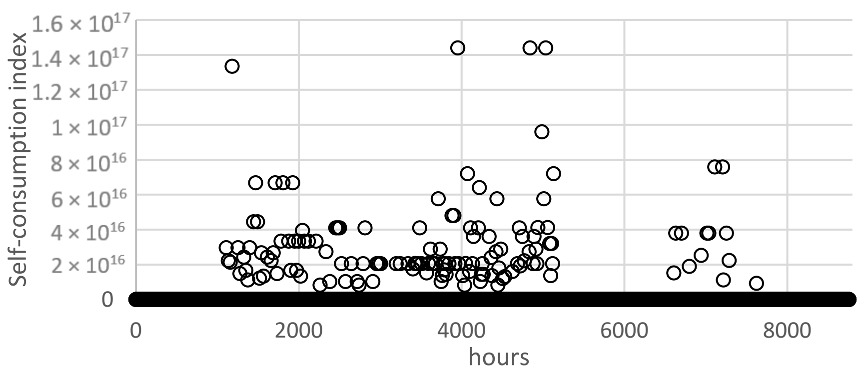

Figure 17. Self-consumption index for a single year.

4. Conclusions

This work looks into the individual and overall performance of a renewable grid-tied 84.5 kWp hybrid system using hourly single-year data from HOMER Pro simulated experiments. An optimal system could be finally determined among different configurations of solar, biomass, diesel generator, chemical storage, and utility grid. The optimized system includes biomass and solar with utility grid connection. Photovoltaic panels, as well as biogas engines, are used to utilize the renewable resources to generate electricity from the sun as well as methane from organic waste. The analysis in this work seeks to study the energy utilization rate and renewable resources PV and biomass power output by using the indices required to examine the entire performance analysis of the renewable hybrid system. As a conclusion of this work, the efficiency of each component was determined; e.g., the converter efficiency of the inverter was predefined. HOMER Pro is used to evaluate the component capacity at a high system efficiency of about 0.97. The solar system PR in June in a hybrid system ranges from 20% to 40%, while it records between 5% and 10% in January. In all seasons, the PR does not exceed 40%. The capacity factor reaches 99% in summer, however in the winter, it remains below 81% and primarily stays between 0% and 32%. It is noteworthy that the rated wattage of the photovoltaic panels that were used in calculating the nominal parameters, performance ratio, and capacitance factors of the hybridization approach is the maximum value achieved in the HOMER results, not the nominal value of the solar module in its database. Renewable penetration is a sufficient parameter to define the renewable capacity compared to the load served over a certain time period. The analyzed system balance (BOS) is evaluated to ensure that the input energy conditions and economic criteria are satisfied. The usage factor (UF) is equal to the 1.03 and 0.972 in January and August, respectively, which is expressed as the overall efficiency of BOS. The use of indices, which comprised of technical and economic variables, to build the system and estimate the capabilities required for its essential components, thereby boosting the system's performance, has been demonstrated. It is worth noting that the specific fuel value has a major effect in the bio-energy efficiency component, while the solar radiation has an efficient impact in the PV system performance analysis. In terms of inverter capacity, it is also advisable to boost the inverter wattage capacity if possible, as this increases the overall PV solar system performance. The component's efficiency is in sync with the system's overall efficiency as the energy produced by each component is proportional to its input energy. We can conclude that HOMER is reliant on component efficiencies provided as inputs, as well as a match between the consumption and production energy, using renewable resources to the greatest extent possible while trading off the economic criteria. In the optimum solution, technical issues such as connections, cabling, and installation were implicitly concerned by the components' efficiencies. In conclusion, in hybrid systems, the performance indices vary throughout the life span of the project. In this work the maximum values were scored in the summer. The performance ratio did not exceed 40%, the capacity factor reached 99%, and the renewable penetration was 497%.

Author Contributions: Conceptualization, H.A.-N.; Methodology, H.A.-N.; Project administration, C.P.; Supervision, C.P.; Validation, C.P.; Visualization, H.A.-N. and C.P.; Writing—original draft, H.A.-N.; Writing—review & editing, C.P., R.A.A. and H.J.E.-K. All authors have read and agreed to the published version of the manuscript.

Funding: This research was funded by Austrian Development Agency and Appear scholarship, grant number ICM-2019-13718. Supported by BOKU Vienna Open Access Publishing Fund.

Acknowledgments: The financial support from the Austrian Development Agency is gratefully acknowledged: Appear project155—MakingEnergy4Palestine (Developing maker-movement-inspired training courses on renewable energy sources in the Gaza Strip) as well as Appear scholarship (Reference number ICM-2019-13718).

Conflicts of Interest: The authors declare no conflict of interest.

References

1. Ismaila, K.G.; Sahin, A.Z.; Yilbas, B.S.; Al-Sharafi, A. Thermo-economic optimization of a hybrid photovoltaic and thermoelectric power generator using overall performance index. *J. Therm. Anal. Calorim.* **2021**, *144*, 1815–1829. [CrossRef]
2. Sawle, Y.; Gupta, S.; Bohre, A.K. Review of hybrid renewable energy systems with comparative analysis of off-grid hybrid system. Renew. *Sustain. Energy Rev.* **2018**, *81*, 2217–2235. [CrossRef]
3. Ayodele, E.; Misra, S.; Damasevicius, R.; Maskeliunas, R. Hybrid microgrid for microfinance institutions in rural areas—A field demonstration in West Africa. *Sustain. Energy Technol. Assess.* **2019**, *35*, 89–97. [CrossRef]
4. Rad, M.A.V.; Ghasempour, R.; Rahdan, P.; Mousavi, S.; Arastounia, M. Techno-economic analysis of a hybrid power system based on the cost-effective hydrogen production method for rural electrification, a case study in Iran. *Energy* **2020**, *190*, 116421. [CrossRef]
5. Mustafi, N.N.; Raine, R.R.; Bansal, P.K. The Use of Biogas in Internal Combustion Engines: A Review. In Proceedings of the ASME 2006 Internal Combustion Engine Division Spring Technical Conference, Aachen, Germany, 7–10 May 2006; pp. 225–234.
6. Jiang, Y.H.; Xiong, S.S.; Shi, W.; He, W.H.; Zhang, T.; Lin, X.K.; Gu, Y.; Lv, Y.D.; Qian, X.J.; Ye, Z.Y.; et al. Research of Biogas as Fuel for Internal Combustion Engine. In Proceedings of the 2009 Asia-Pacific Power and Energy Engineering Conference, Wuhan, China, 28–31 March 2009; pp. 1–4.
7. Rashid, F.; Hoque, E.; Aziz, M.; Sakib, T.N.; Islam, T.; Robin, R.M. Investigation of Optimal Hybrid Energy Systems Using Available Energy Sources in a Rural Area of Bangladesh. *Energies* **2021**, *14*, 5794. [CrossRef]
8. Benato, A.; Macor, A.; Rossetti, A. Biogas Engine Emissions: Standards and On-Site Measurements. *Energy Procedia* **2017**, *126*, 398–405. [CrossRef]
9. Al-Najjar, H.; El-Khozondar, H.J.; Pfeifer, C.; Al Afif, R. Hybrid grid-tie electrification analysis of bio-shared renewable energy systems for domestic application. *Sustain. Cities Soc.* **2022**, *77*, 103538. [CrossRef]
10. Zhang, C.; Sun, J.; Ma, J.; Xu, F.; Qiu, L. Environmental Assessment of a Hybrid Solar-Biomass Energy Supplying System: A Case Study. *Int. J. Environ. Res. Public Health* **2019**, *16*, 2222. [CrossRef]
11. Bartolucci, L.; Cordiner, S.; Mulone, V.; Rocco, V.; Rossi, J.L. Hybrid renewable energy systems for renewable integration in microgrids: Influence of sizing on performance. *Energy* **2018**, *152*, 744–758. [CrossRef]
12. Decker, B.; Jahn, U. Performance of 170 grid connected PV plants in Northern Germany—Analysis of yields and optimization potentials. *Sol. Energy* **1997**, *59*, 127–133. [CrossRef]
13. Teo, Y.L.; Go, Y.I. Techno-economic-environmental analysis of solar/hybrid/storage for vertical farming system: A case study, Malaysia. *Renew. Energy Focus* **2021**, *37*, 50–67. [CrossRef]
14. Zebra, E.I.C.; van der Windt, H.J.; Nhumaio, G.; Faaij, A.P. A review of hybrid renewable energy systems in mini-grids for off-grid electrification in developing countries. *Renew. Sustain. Energy Rev.* **2021**, *144*, 111036. [CrossRef]
15. Ma, T.; Yang, H.; Lu, L. Long term performance analysis of a standalone photovoltaic system under real conditions. *Appl. Energy* **2017**, *201*, 320–331. [CrossRef]
16. Khalid, A.; Mitra, I.; Warmuth, W.; Schacht, V. Performance ratio—Crucial parameter for grid connected PV plants. *Renew. Sustain. Energy Rev.* **2016**, *65*, 1139–1158. [CrossRef]
17. Reich, N.; Müller, B.; Armbruster, A.; van Sark, W.; Kiefer, K.; Reise, C. Performance ratio revisited: Is PR > 90% realistic? *Prog. Photovolt. Res. Appl.* **2012**, *20*, 717–726. [CrossRef]
18. Ozerdem, O.C.; Tackie, S.; Biricik, S. Performance evaluation of Serhatkoy (1.2 MW) PV power plant. In Proceedings of the 2015 9th International Conference on Electrical and Electronics Engineering (ELECO), Bursa, Turkey, 26–28 November 2015; pp. 398–402.
19. Barua, S.; Prasath, R.A.; Boruah, D. Rooftop Solar Photovoltaic System Design and Assessment for the Academic Campus Using PVsyst Software. *Int. J. Electron. Electr. Eng.* **2017**, *5*, 76–83. [CrossRef]
20. Nafreen, M.; Hossen, I.; Rahman, A.; Islam, R.; Ferdous, Z.; Sohag, S.H. 100KW Rooftop Solar Photovoltaic Power Plant: Block "B" of Ahsanullah University of Science and Technology. *IOSR J. Electr. Electron. Eng.* **2017**, *12*, 1–4. [CrossRef]
21. Zabalaga, P.J.; Cardozo, E.; Campero, L.A.C.; Ramos, J.A.A. Performance Analysis of a Stirling Engine Hybrid Power System. *Energies* **2020**, *13*, 980. [CrossRef]
22. NASA. *Surface Meteorology and Solar Energy*; NASA: Washington, DC, USA, 2020.
23. MDLF—Municiple Development and Lending Fund. *MDLF Annual/Semi Annual Reports*; MDLF: Al-Bireh, Palestine, 2019.
24. Abbood, A.A.; Salih, M.A.; Mohammed, A.Y. Modeling and simulation of 1 mw grid connected photovoltaic system in Karbala city. *Int. J. Energy Environ.* **2018**, *9*, 153–168.
25. Cabrera-Tobar, A.; Bullich-Massagué, E.; Aragüés-Peñalba, M.; Gomis-Bellmunt, O. Topologies for large scale photovoltaic power plants. *Renew. Sustain. Energy Rev.* **2016**, *59*, 309–319. [CrossRef]
26. IS/IEC. Photovoltaic System Performance Monitoring—Guidelines For Measurement, Data Exchange and Analysis. In *Indian Standard IS/IEC 61724: 1998*; IS/IEC: Geneva, Switzerland, 2010.
27. Al-Najjar, H.; Pfeifer, C.; Al Afif, R.; El-Khozondar, H.J. Estimated View of Renewable Resources as a Sustainable Electrical Energy Source, Case Study. *Designs* **2020**, *4*, 32. [CrossRef]
28. Deng, L.; Liu, Y.; Wang, W. *Biogas Technology*; Springer: Singapore, 2020.

29. Tian, Y.; Zhang, H.; Chai, Y.; Wang, L.; Mi, X.; Zhang, L.; Ware, M.A. Biogas properties and enzymatic analysis during anaerobic fermentation of Phragmites australis straw and cow dung: Influence of nickel chloride supplement. *Biodegradation* **2017**, *28*, 15–25. [CrossRef] [PubMed]
30. Bruni, G.; Cordiner, S.; Mulone, V.; Sinisi, V.; Spagnolo, F. Energy management in a domestic microgrid by means of model predictive controllers. *Energy* **2016**, *108*, 119–131. [CrossRef]
31. Elnaggar, M.; Edwan, E.; Ritter, M. Wind Energy Potential of Gaza Using Small Wind Turbines: A Feasibility Study. *Energies* **2017**, *10*, 1229. [CrossRef]
32. Adaramola, M.S.; Agelin-Chaab, M.; Paul, S.S. Analysis of hybrid energy systems for application in southern Ghana. *Energy Convers. Manag.* **2014**, *88*, 284–295. [CrossRef]
33. Jahn, U.; Niemann, M.; Blaesser, G.; Dahl, R.; Castello, S.; Clavadetscher, L.; Faiman, D.; Mayer, D.; van Otterdijk, K.; Sachau, J.; et al. International energy agency TASK II database on photovoltaic power systems: Statistical and analytical evaluation of PV operational data. In Proceedings of the 15th European Photovoltaic Solar Energy Conference, Vienna, Austria, 6–10 July 1998.
34. Nurdiana, E.; Subiyanto, I.; Indarto, A.; Riza; Wibisono, G.; Hudaya, C. Performance analysis and evaluation of a 10.6 kWp grid-connected photovoltaic system in Serpong. *IOP Conf. Ser. Mater. Sci. Eng.* **2020**, *909*, 012019. [CrossRef]